Molecular Cell, Vol. 20, 187–198, October 28, 2005, Copyright ©2005 by Elsevier Inc. DOI 10.1016/j.molcel.2005.09.022

Recognition of RNA Polymerase II and Transcription Bubbles by XPG, CSB, and TFIIH: Insights for Transcription-Coupled Repair and Cockayne Syndrome

Altaf H. Sarker,[1,4] Susan E. Tsutakawa,[1,4] Seth Kostek,[2] Cliff Ng,[1] David S. Shin,[3] Marian Peris,[2] Eric Campeau,[1,5] John A. Tainer,[1,3] Eva Nogales,[1,2] and Priscilla K. Cooper[1,*]

[1]Life Sciences Division
Lawrence Berkeley National Laboratory
1 Cyclotron Road
Mail Stop 74R157
Berkeley, California 94720

[2]Howard Hughes Medical Institute
Department of Molecular and Cell Biology
University of California, Berkeley
Berkeley, California 94720

[3]Department of Molecular Biology and
The Skaggs Institute for Chemical Biology
The Scripps Research Institute
La Jolla, California 92037

Summary

Loss of a nonenzymatic function of XPG results in defective transcription-coupled repair (TCR), Cockayne syndrome (CS), and early death, but the molecular basis for these phenotypes is unknown. Mutation of CSB, CSA, or the TFIIH helicases XPB and XPD can also cause defective TCR and CS. We show that XPG interacts with elongating RNA polymerase II (RNAPII) in the cell and binds stalled RNAPII ternary complexes in vitro both independently and cooperatively with CSB. XPG binds transcription-sized DNA bubbles through two domains not required for incision and functionally interacts with CSB on these bubbles to stimulate its ATPase activity. Bound RNAPII blocks bubble incision by XPG, but an ATP hydrolysis-dependent process involving TFIIH creates access to the junction, allowing incision. Together, these results implicate coordinated recognition of stalled transcription by XPG and CSB in TCR initiation and suggest that TFIIH-dependent remodeling of stalled RNAPII without release may be sufficient to allow repair.

Introduction

Besides threatening genomic integrity, DNA damage more immediately obstructs transcription and replication. Elongating RNA polymerase (RNAP) can be blocked by DNA lesions in the transcribed strand (Svejstrup, 2003; Tornaletti and Hanawalt, 1999). Left uncorrected, the block can lead to reduced transcription of critical genes and acts as a potent signal for apoptosis and induction of the p53 response (Ljungman and Lane, 2004). The evolutionarily conserved process of TCR counteracts these effects by preferentially removing blocking lesions from transcribed strands (TS) of active genes as compared to the corresponding nontranscribed strands (NTS) or the genome overall. TCR is likely initiated by more efficient recognition of stalled RNAP than of the lesion itself, but it has generally been assumed that an essential early step in the process is removal of the arrested polymerase to allow repair to proceed (Svejstrup, 2002). Although the molecular mechanism of TCR in mammals is unknown, gene products important for it have been identified through involvement in the hereditary disorder CS. This disorder shares extreme sun sensitivity but few other clinical features with xeroderma pigmentosum (XP) (Berneburg and Lehmann, 2001; Lehmann, 2003; Rapin et al., 2000), which primarily involves defects in nucleotide excision repair (NER), a generalized repair process that removes and replaces segments of DNA containing UV damage and other bulky lesions throughout the genome (Hoeijmakers, 2001).

CS is a rare postnatal developmental disorder involving severe physical and mental retardation and pronounced cachexia, typically causing death in childhood. Cells from CS patients are UV sensitive and fail to recover RNA synthesis after UV despite evidently normal repair of lesions in the genome overall (Mayne and Lehmann, 1982). These features led to the discovery of TCR in normal cells and its absence in CS cells (Mellon et al., 1987; van Hoffen et al., 1993). In contrast, the clinical features of XP include severe sunlight-induced skin changes and a very high incidence of skin cancers. Global genome repair (GGR) of UV-induced lesions is absent in cells from classical XP patients who have inactivating mutations in any of seven genes (*XPA–XPG*) required for NER. CS is most frequently the result of mutations in either of two genes, *CSB* and *CSA*, not involved in NER but required for TCR. However, rare mutations in any of three genes required for NER—*XPB*, *XPD*, and *XPG*—can result in clinical CS in addition to XP, with XP-D and XP-G patients being especially heterogeneous.

Properties of CSB implicate it in initiation of TCR through recognition of stalled RNAP and recruitment of other TCR components. It is a member of the SWI2/SNF2 family of DNA-dependent ATPases and is found in cellular complexes with both RNA polymerases I and II (Bradsher et al., 2002; van Gool et al., 1997). CSB binds RNAPII arrested at a template lesion in vitro and recruits TFIIH (Tantin, 1998), an essential ten-subunit complex that includes the DNA helicases XPB and XPD and is required for both transcription initiation and NER as well as TCR (Coin and Egly, 1998). The DNA-dependent ATPase activity of CSB has been linked to chromatin remodeling activity in vitro (Citterio et al., 2000), and ATPase domain mutations strongly reduce CSB function in post-UV recovery of RNA synthesis, an indicator for TCR (Citterio et al., 1998; Selzer et al., 2002).

The roles of TFIIH and XPG in NER are well understood, but the nature of their separable roles in TCR remains to be elucidated. Both the XPB and XPD heli-

*Correspondence: pkcooper@lbl.gov
[4]These authors contributed equally to this work.
[5]Present address: University of Massachusetts Medical School, Program in Gene Function and Expression, Worcester, Massachusetts, 01605.

case components of TFIIH are required in NER to open an approximately 30 nt bubble in the DNA around the lesion (Evans et al., 1997b). The bubble then forms the substrate for incision by the structure-specific nucleases XPG and ERCC1/XPF. XPB is uniquely required for transcription initiation as well as for NER and TCR, so only very conservative *xpb* mutations can be tolerated, and, furthermore, it is not clear what distinguishes the nature or location of the few *xpd* mutations that result in CS from those that result in XP (Lehmann, 2001). Analysis of patient mutations in *XPG* has been somewhat more informative, revealing that conservative mutations that inactivate its endonuclease function but produce full-length protein result only in NER defects and mild XP, whereas mutations that severely truncate the protein result in a profound form of CS (XP-G/CS), with death in infancy or early childhood (Emmert et al., 2002; Lalle et al., 2002; Nouspikel et al., 1997). This fact suggests that a noncatalytic function of XPG is necessary for normal postnatal development. This conclusion is confirmed by mouse models, as *xpg* knockouts exhibit a severe CS-like phenotype and death by 21 days (Harada et al., 1999), whereas mice lacking NER due to point mutations that inactivate the XPG endonuclease are essentially normal except for hypersensitivity to UV (Shiomi et al., 2004; Tian et al., 2004). However, the nature of this vital noncatalytic function of XPG is unknown.

To elucidate the nonenzymatic function of XPG that is essential postnatally and its relationship to TCR, we characterized the interaction of XPG with RNAPII, transcription-sized DNA bubbles, CSB, and stalled transcription elongation complexes. The presented experimental results provide insights into the mechanism by which TCR is initiated and suggest roles for XPG and TFIIH in TCR, with implications for the causal nature of particular *xpg* mutations in postnatal developmental failure and mortality in an extreme form of Cockayne syndrome.

Results

Interaction of XPG with RNAPII

To investigate whether XPG might be involved in the recognition step of TCR, we asked whether XPG interacts physically with RNAPII. By using two different XPG antibodies (R1 and R2), we consistently observed that RNAPII coimmunoprecipitated with XPG from HeLa nuclear extracts prepared from undamaged cells (Figure 1A). Interestingly, the RNAPII that coimmunoprecipitated was the hyperphosphorylated IIo form primarily associated with elongation complexes (Laybourn and Dahmus, 1990), although both it and the hypophosphorylated IIa form were present in the nuclear extract. The converse, coimmunoprecipitation of XPG with an antibody against the large subunit of RNAPII, was not observed. However, by mixing together purified proteins, we found that the RNAPII antibody could reciprocally coimmunoprecipitate XPG, and an XPG antibody pulled down both RNAPIIo and IIa (Figure 1B), establishing that neither DNA nor other proteins are required for complex formation and that the phosphorylation state of RNAPII is not a direct determinant of interaction. This result suggests that the preferential coimmunoprecipitation of RNAPIIo with XPG from nuclear extracts is a result of their cellular association. Control reactions (not shown) with the purified proteins demonstrated that the antibodies are not crossreactive.

The interaction of XPG with the elongating form of RNAPII in the cell is consistent with the idea that XPG may function in TCR through independent recognition of stalled RNAPII. To test this possibility, we formed stalled ternary complexes of RNAPII by using an in vitro promoterless transcription initiation system, which results in highly processive transcription that maintains the transcription bubble in the ternary complex (Sidorenkov et al., 1998). In this approach, RNAPII is bound to a 9- or 10-mer RNA primer hybridized to the TS, and the NTS is then added to form a transcription bubble. Transcription from the RNA primer is initiated by the addition of ribonucleotide triphosphates (Figure 1C). To stall transcription by encountering a bulky lesion, we introduced a cisplatin (cis-Pt) intrastrand crosslink in the TS at a unique GTG sequence 30 nt downstream from the 3′ end of the primer (see Figure S1 in the Supplemental Data available with this article online). Transcription of this template with no lesion generated a 61 nt runoff transcript, whereas all transcripts from the lesion-containing template terminated at 39 nt, corresponding to the position of the cis-Pt plus the 10 nt primer (Figure 1D). The ternary complex formed by the labeled RNA product, DNA, and the stalled RNAPII was visualized by an electrophoretic mobility shift assay (EMSA; Figure 1E, lane 1). Both RNAPIIo and IIa actively elongate in this in vitro system, in contrast to the situation in the cell. CSB formed a complex with both forms of stalled RNAPII as evidenced by decreased mobility in the EMSA (lane 2), as previously reported with a C-tailed transcription-initiation system (Tantin et al., 1997). Significantly, XPG alone also produced a supershift of both ternary complexes (lane 4). Furthermore, XPG and CSB together led to a larger decrease in mobility (lane 3), demonstrating that XPG, CSB, and the stalled RNAPII can form a supramolecular complex. These findings suggest a role for XPG in initiation of TCR through recognition of stalled RNAPII.

Because XPG and RNAPIIo coimmunoprecipitated from extracts of undamaged cells, the TCR machinery may also recognize RNAPII stalled by means other than an encounter with a lesion. This was tested by using a template with an A-less cassette (Figure 1C; Figure S1), so that transcription without UTP results in stalling at the first template A due to nucleotide deprivation, giving a 43 nt product (Figure 1F). As with transcription stalled by a cis-Pt lesion, both CSB and XPG interacted with the halted ternary complex, as shown by reduced mobility in EMSA, and together they formed a supracomplex (Figure 1G). Similar EMSA results were obtained for RNAPII halted by nucleotide deprivation in a C-tailed initiation system (Figures S2C and S2D). We examined the importance of the transcription bubble itself by initiating transcription on the A-less cassette template in the absence of the NTS, a condition that allows elongation in this system but with significantly lower processivity (Kireeva et al., 2000). A halted RNAPIIa ternary complex was observed, although of lower intensity consistent with decreased transcription effi-

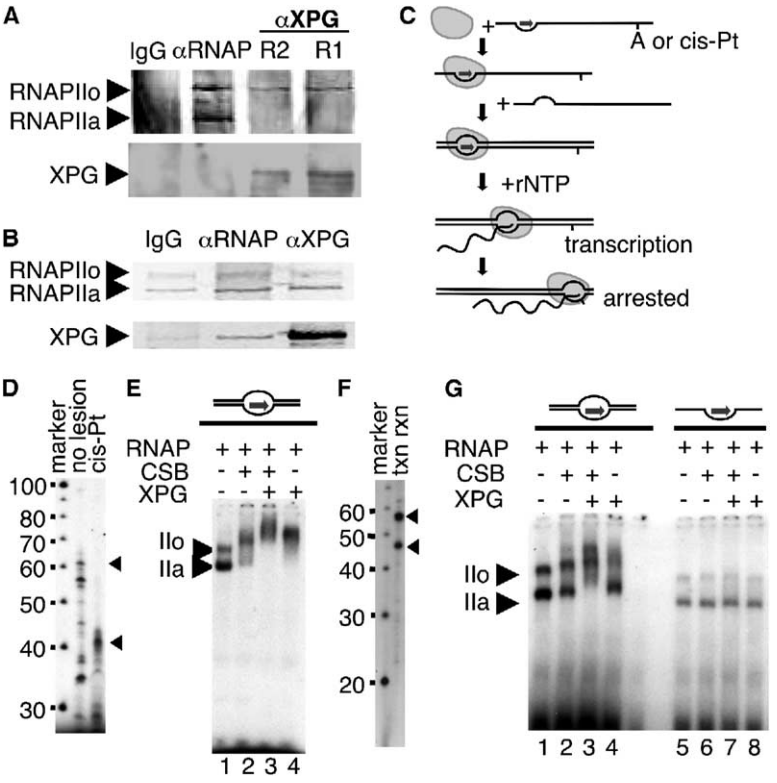

Figure 1. XPG Interactions with RNAPII

(A) Western blotting analysis showing coimmunoprecipitation of hyper- (IIo), but not hypo- (IIa), phosphorylated forms of RNAPII with XPG from undamaged HeLa cells. Nuclear extracts were incubated with RNAPII antibody or antibodies R1 or R2 against distinct regions in the R-domain of XPG. Immunoprecipitates were probed for XPG and RNAPII.

(B) Western blotting analysis showing that purified XPG and both forms of RNAPII interact directly. XPG (300 ng) and RNAPII (5 μg) were mixed and coimmunoprecipitated with mouse IgG, XPG C-term antibody 8H7, or RNAPII antibody Sc-899.

(C) Schematic for formation of a stalled elongation complex. A 9- or 10-mer primer RNA was hybridized to the TS (sequences in Figure S1). Purified human RNAPII was bound to the RNA/DNA hybrid, and addition of the NTS formed a transcription bubble (Sidorenkov et al., 1998). Elongation of the RNA primer occurred upon addition of ribonucleotide triphosphates. Transcription was stalled either by a cis-Pt lesion at nt 30–32 or by UTP nucleotide deprivation with a 34 nt A-less cassette.

(D) Denaturing gel of RNA transcripts from substrate without or with cis-Pt, indicating that RNAPII ran to the end the substrate without a lesion (although with numerous pause sites) but stalled at the cis-Pt lesion. The RNA product was labeled by incorporation of [α^{32}P]-GTP and visualized by phosphorimaging. Positions of the runoff 61 nt transcript (including 10-mer primer) and the 39 nt transcript (including primer) terminated at the lesion are indicated by arrows.

(E) EMSA of RNAPII stalled at a cis-Pt lesion showing supracomplex formation when incubated with XPG and/or CSB. Both RNAPIIo and IIa actively transcribe in this system.

(F) Denaturing gel of transcription reaction (txn rxn) products from the substrate containing an A-less cassette. In the presence of [α^{32}P]-CTP, ATP, and GTP but absence of UTP, RNAPII either stopped at the first A (43 nt including 9-mer primer) or ran to the end of the DNA template (59 nt including primer), as indicated by arrows.

(G) EMSA showing formation of supracomplexes of XPG and/or CSB with RNAPII ternary complexes stalled by nucleotide deprivation (left). These complexes did not form with RNAPII stalled during transcription without the NTS (right).

ciency (Figure 1G, lane 5), whereas RNAPIIo was apparently inactive under these conditions. Neither CSB nor XPG appreciably shifted the RNAPIIa complex formed without the NTS (lanes 6–8). These results suggest that recognition of stalled RNAPII by either XPG or CSB is independent of a lesion and may include interactions with the transcription bubble.

Stable and Specific Binding of XPG to Transcription-Sized DNA Bubbles

To test for specific interactions of XPG with transcription bubbles in DNA, we compared binding of XPG to synthetic bubble DNA substrates of varying length (5, 10, 15, 20, and 30 nt; Figure S1) in the presence of poly(dI:dC) to eliminate nonspecific binding. Under these conditions, no binding is observed to dsDNA (not shown). For all DNA-bubble sizes shown, a defined band shift was observed by EMSA (Figure 2B; quantified in Figure S3A). XPG showed a strong binding preference for DNA bubbles whose size resembled those associated with transcription, which are 14–22 nt long in eukaryotic elongation complexes (Fiedler and Timmers, 2001). At the highest concentration of XPG, binding to transcription-sized bubbles of 10–20 nt in length was approximately 2-fold greater than to the 30 nt bubble (which corresponds to the substrate for incision during NER), with an even stronger preference at lower XPG concentrations.

To determine the affinity of XPG for 10 nt DNA bubbles, we measured binding as a function of increasing XPG concentration in the absence of poly(dI:dC) (Figure S3B). Based on a Hill plot (Figure S3C), XPG binds bubble DNA tightly with an affinity of 10.3 nM. Binding was extremely rapid and saturated within one minute (not shown). To characterize the dissociation kinetics, we incubated XPG with labeled 10 nt bubble DNA for one minute and then added unlabeled 10 nt bubble DNA as a competitor. XPG did not release the DNA for at least 1 hr even in the presence of a 5-fold higher competitor concentration (Figure 2C). Thus, the XPG:DNA bubble complex forms rapidly and is extremely stable. XPG can bind to half-bubbles or splayed-arm substrates (Hohl et al., 2003), but the preferred DNA binding substrate has not previously been determined. To define what structural elements of the DNA bubble are recognized, a competition assay was performed in which XPG was added to a mixture of labeled 10 nt bubble DNA and one of the following unlabeled substrates: 10 nt bubble DNA, ssDNA, dsDNA, a 5′ flap-gap DNA, or a splayed-arm substrate. Comparison of the amounts

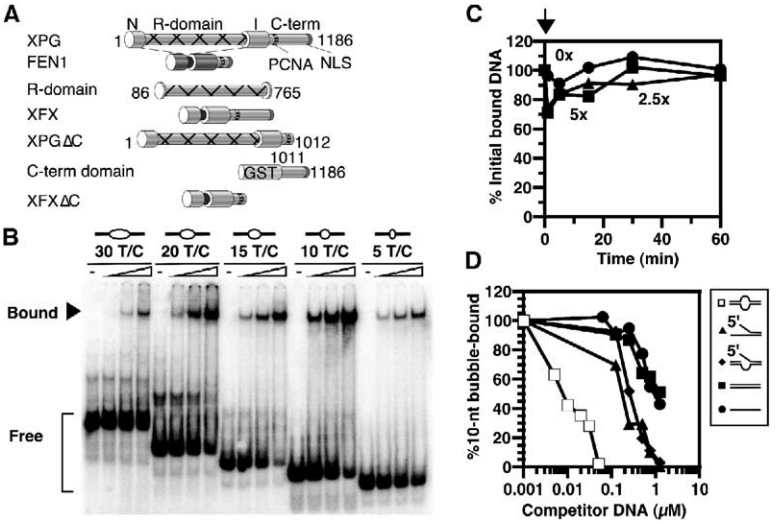

Figure 2. XPG Binds Transcription-Sized DNA Bubbles

(A) Schematic model of XPG and FEN1 domain organization and of the XPG domain or deletion constructs. Catalytic domains (N, I), PCNA binding motif, and nuclear localization signal (NLS) are shown. In XFX, the R-domain was replaced by the corresponding FEN1 linker. The C-terminal domain of XPG was deleted in XPGΔC, and both the R- and C-terminal domains were removed in XFXΔC. The C-terminal domain alone was expressed as a GST fusion.

(B) EMSA showing binding of XPG to DNA bubbles of various sizes. XPG at increasing concentrations (0, 40, 80, and 160 nM) was incubated with labeled DNA substrate (5 nM), and bound and free DNA were separated by native PAGE. Quantification is in Figure S2A.

(C) Quantification of results from an EMSA (not shown) demonstrating stability of XPG binding to 10 nt DNA bubbles. XPG (80 nM) was incubated with labeled 10 nt bubble DNA (5 nM), challenged with indicated concentrations of unlabeled DNA after 1 min (arrow), and samples taken at various times.

(D) Quantification of results from an EMSA competition study (not shown) establishing specificity of XPG for two-junction DNA bubbles. XPG (40 nM) was incubated with labeled 10 nt bubble DNA (5 nM) in the presence of unlabeled DNA competitors: 10 nt bubble DNA (□), ssDNA (●), dsDNA (■), 5′ flap gap DNA (♦), and splayed arm DNA (▲).

of unlabeled DNA needed to reduce binding to the labeled 10 nt bubble by 50% reveals that XPG preferentially bound the bubble DNA by ~150-fold greater than dsDNA, ~120-fold greater than ssDNA, and 20- to 30-fold greater than the single junction substrates (Figure 2D). The striking preference for the bubble as opposed to its separate elements suggests that for stable binding, XPG recognizes the entire bubble rather than ssDNA to dsDNA transitions at one junction.

DNA Bubble Binding and Incision Map to Distinct Regions of XPG

To map the region of XPG required for stable DNA bubble binding, we targeted regions outside of the N and I nuclease subdomains, which are conserved with flap endonuclease-1 (FEN1) and harbor catalytically important residues (Figure 2A) (Constantinou et al., 1999; Harrington and Lieber, 1994). FEN1 is also a structure-specific endonuclease that cleaves at ss/ds junctions with the same polarity as XPG, but it requires a 5′-ss terminus and is unable to incise bubble structures (Wu et al., 1996). Compared to FEN1, XPG has large insertions between the N and I catalytic domains and also at the C terminus of the protein (Figure 2A). The insertion between the N and I regions in XPG is a unique sequence of approximately 600 residues that we term the R (recognition)-domain and that has been referred to by others as the spacer region (Thorel et al., 2004). X-ray crystal structures reveal that the analogous region between the N and I subdomains in FEN1 corresponds to a flexible loop of only 47 residues (Hosfield et al., 1998). In addition, the XPG C terminus encoded by exon 15 (C-terminal domain) has diverged from the FEN1 C terminus by the addition of roughly 145 residues and, moreover, is not present in RAD2, the *S. cerevisiae* homolog of XPG (Shiomi et al., 2005).

To determine whether its unique R-domain and C-terminal domain are important for stable interaction between XPG and DNA, we examined the effect of antibodies against these regions on bubble DNA binding (Figure 3A). Addition of the R-domain antibody R2 led to a concentration-dependent decrease in the amount of shifted DNA (Figure 3A, compare lanes 4 and 5 to lane 2), with binding essentially eliminated at the highest antibody concentration, suggesting that binding of this R-domain antibody to XPG precludes bubble DNA binding. Addition of preimmune sera (Figure 3A, lane 6) or BSA (Figure 3A, lane 7) had no effect. In contrast, addition of the 8H7 monoclonal antibody that recognizes an epitope in the C-terminal domain resulted in a supershift of the XPG bound DNA (Figure 3A, lane 3), confirming that the shifted complex contains XPG protein and suggesting that the epitope recognized by this antibody is not essential for bubble DNA binding. However, the amount of XPG bound DNA was reduced by the 8H7 antibody, consistent with some steric hindrance (Figure 3A, compare lanes 2 and 3).

To directly test involvement of these domains in DNA bubble recognition, we designed two XPG constructs with these regions deleted (Figure 2A): a chimera (XFX) in which the XPG R-domain was replaced by a corresponding FEN1 loop, and XPG lacking the C-terminal domain (XPGΔC). Both XFX and XPGΔC specifically incised a 30 nt DNA bubble substrate at the same position near the 3′ end of the bubble as does full-length XPG (Figure 3B). The incision activity of XFX was weaker than that of XPG, in qualitative agreement with reduced incision activity recently reported for XPG proteins having large deletions in the R-domain (Dunand-Sauthier et al., 2005). Interestingly, however, the XFX chimeric protein also makes a specific alternate incision further away from the 3′ junction of the bubble with similar frequency (P2 in Figure 3B). When both the proper incision product and the alternate product P2 are considered, the rate of incision by XFX is about 80% of that for full-length XPG. In contrast, XPGΔC has

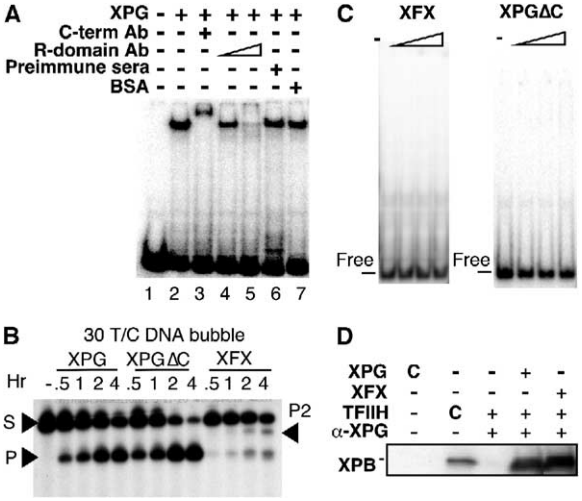

Figure 3. DNA Binding, but Not Incision, Requires R- and C-Terminal Domains

(A) EMSA showing the effect of R-domain and C-terminal domain antibodies on XPG binding to 10 nt bubble DNA. XPG (80 nM) was preincubated alone, with 1 μg C-terminal domain antibody (XPG antibody 8H7), with 0.8 or 1.6 μg R2 peptide antibody, with 10 μg preimmune sera, or with 10 μg BSA. Binding assays were performed as in Figure 2B.

(B) Denaturing PAGE showing incision by XPG, XPGΔC, or XFX. Proteins (5 nM) were incubated for times up to 4 hr with 30 nt bubble DNA (33 nM) as substrate (S) to give incised product (P). A second incision product (P2) was observed in XFX reactions.

(C) EMSA showing lack of detectable DNA binding by XPG constructs lacking R-domain or the C-terminal domain. XFX (57, 114, and 172 nM) or XPGΔC (40, 80, and 120 nM) was incubated with 15 nt bubble DNA (5 nM) and analyzed as in Figure 2B.

(D) Coimmunoprecipitation studies showing TFIIH interaction with XPG and XFX. Purified proteins were mixed and immunoprecipitated with XPG antibody 8H7. TFIIH was detected by Western blotting analysis with an antibody against XPB. The input proteins were loaded separately as controls, "C".

substantially greater incision activity than full-length XPG under conditions of substrate excess (Figure 3B; A.S., unpublished data). The retention of incision of bubble DNA by XFX and XPGΔC establishes that neither the R-domain nor the C-terminal domain is essential for the catalytic function of XPG. Strikingly, however, neither protein is competent for binding to DNA bubbles, as observed by EMSA (shown for the 15 nt bubble in Figure 3C). These results establish a requirement for both the R- and C-terminal domains of XPG in stable bubble DNA binding, but not for incision of DNA bubble structures, and demonstrate that these two functions of XPG are physically and functionally separate capabilities.

Although the R-domain is not required for incision by XPG, it is essential for NER activity both in vitro and in vivo (Dunand-Sauthier et al., 2005; Thorel et al., 2004). This requirement has been attributed to the lack of interaction with TFIIH in the cell by XPG constructs lacking portions of the R-domain. However, we determined that purified human TFIIH can be coimmunoprecipitated with XFX to the same extent as with full-length XPG under physiological salt conditions (Figure 3D). We conclude that the R-domain is not essential for direct protein-protein interaction between XPG and TFIIH and that some other function of XPG not directly related to TFIIH binding is disrupted by R-domain mutations in cells.

XPG Stimulates CSB Binding to Bubble DNA and CSB ATPase Activity

Having found that XPG preferentially binds transcription-sized DNA bubbles and forms a supracomplex with CSB on stalled RNAPII, we tested whether CSB binding to bubble DNA and its DNA-dependent ATPase activity are affected by XPG. CSB alone bound 10 nt DNA bubble substrates in the absence of ATP to give two minor bands in an EMSA as well as a diffuse shift of the DNA substrate throughout the entire lane (Figure 4A), consistent with a weak CSB-bubble DNA interaction. Addition of XPG stabilized this interaction and supershifted the complex. In the presence of XPG at the highest concentration of CSB, there was a 60% increase in the amount of bound DNA compared to that with either protein alone, indicating that XPG and CSB bind cooperatively. Antibodies against either XPG or the HA-tagged CSB protein further decreased the mobility of the complex, confirming that both proteins are present in the supershifted band (Figure 4B). The interaction is specific, as BSA did not produce a supershift. These results indicate that XPG and CSB cooperatively form a stable complex with transcription-sized DNA bubbles.

We have confirmed and extended a previously reported direct interaction between XPG and CSB (Iyer et al., 1996) by both Far Western blotting analysis of purified proteins (Figure 4D and data not shown) and coimmunoprecipitation after expression in insect cells (not shown). To assess the functional significance of the interaction, we quantified the ATPase activity of CSB in the presence of either dsDNA or 10 nt bubble DNA, with or without XPG. Consistent with previous studies (Christiansen et al., 2003; Citterio et al., 1998), the ATPase of CSB was more active in the presence of bubble DNA than dsDNA, with the initial rate being over 2-fold higher (Figure 4C; Figure S4). Significantly, XPG enhanced the bubble DNA-dependent ATPase activity of CSB approximately 2-fold but had no effect on dsDNA-dependent activity (Figure 4C). As expected, XPG alone lacked ATPase activity (data not shown). We mapped the domain of XPG that interacts with CSB by Far Western blotting analysis in which different constructs of XPG (Figure 2A) were probed with CSB and interaction was detected with CSB antibody. Only XPG constructs containing the C-terminal domain interacted (Figure 4D). Furthermore, a C-terminal GST fusion stimulated the ATPase activity of CSB but XFXΔC did not, confirming that the C-terminal domain of XPG is necessary and sufficient for CSB stimulation (Figure 4E). Because the C-terminal domain is also necessary for bubble binding, we wondered whether the stimulation might be due, nonspecifically, to binding of the ssDNA region of the bubble. Arguing against this possibility, the human ssDNA binding protein RPA did not affect ATPase activity. These results are consistent with cooperative action of XPG and CSB at the transcription bub-

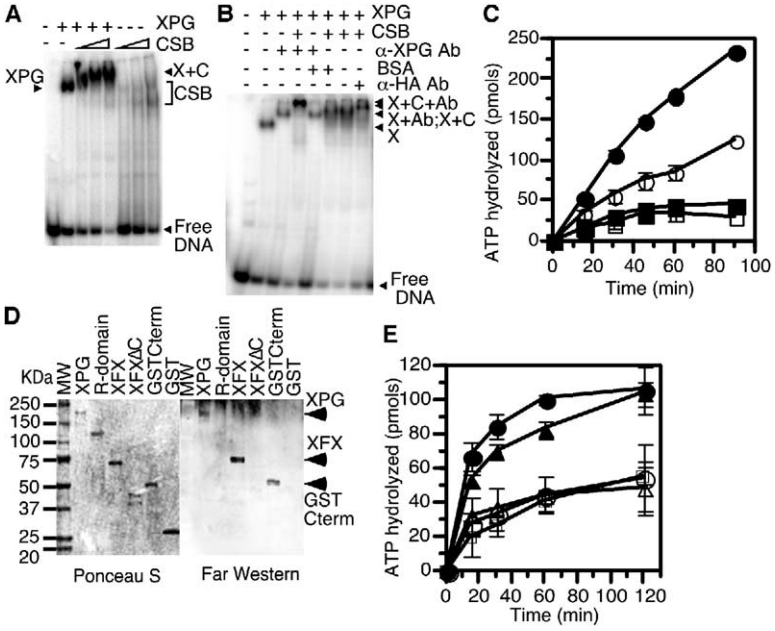

Figure 4. CSB Binding to Bubble DNA and Complex Formation with XPG

(A) EMSA showing cooperative interaction of CSB and XPG on DNA bubbles (arrow). Labeled 10 nt bubble DNA was incubated with increasing concentrations of CSB (0, 60, 120, and 180 nM), XPG (124 nM), or both (X+C).

(B) EMSA demonstrating presence of XPG and CSB in antibody (Ab)-supershifted bands (arrows). A mixture of XPG (82 nM), HA-tagged CSB (89 nM), and labeled 10 nt bubble DNA (5 nM) was incubated with 1 μg XPG antibody (8H7), 1 μg HA tag antibody, or BSA (600 ng).

(C) Quantification of CSB ATPase activity and stimulation by XPG. ATPase activity of CSB (5 nM) incubated with either 10 nt bubble (○, ●) or linear DNA (□, ■) was measured in the absence (open) or presence (filled) of XPG (5 nM) by release of ^{32}P from [γ-^{32}P]-ATP. Error bars represent standard error of the mean as determined from three independent experiments.

(D) Far Western blotting analysis showing interaction with CSB mapped to the C-terminal domain of XPG (arrows). XPG (350 ng), R-domain (750 ng), XFX (500 ng), XFXΔC (480 ng), GST-C-term domain (500 ng), and GST (1 μg) were separated by SDS-PAGE, transferred to nitrocellulose, stained with Ponceau S (left), and incubated with HA-tagged CSB and probed with anti-HA antibody (right).

(E) Quantification of CSB ATPase activity showing that the C-terminal domain of XPG is necessary and sufficient for stimulation. Activity was measured as in (C), either alone (○) or in the presence of full-length XPG (●), GST-C-term domain (▲), XFXΔC (△), or the ssDNA binding control RPA (□). Error bars represent standard error of the mean as determined from three independent experiments.

ble during TCR, mediated through the C-terminal domain of XPG.

Bubble Bound RNAPII Is Remodeled by TFIIH To Allow XPG Incision

The accepted model for TCR is that stalled RNAPII, although providing a very efficient signal for damage recognition, prevents access to the blocking lesion and must somehow be removed in order for repair to occur (Mellon et al., 1987). Indeed, RNAPII stalled at a thymine dimer during in vitro transcription has been shown to prevent access of photolyase, a much smaller protein than the NER incision machinery (Donahue et al., 1994), and the footprint of the stalled RNAPII completely covers the lesion (Selby et al., 1997; Tornaletti et al., 1999). However, other in vitro studies with either nuclear extracts or partially purified or reconstituted incision systems have concluded that dual incision can occur in the presence of stalled RNAPII (Selby et al., 1997; Tremeau-Bravard et al., 2004). To reconcile these discordant observations, we considered the possibility that the conformation of stalled RNAPII might be actively altered to allow repair. Because CSB was not required for the incisions observed at blocked transcription (Selby et al., 1997; Tremeau-Bravard et al., 2004), the hypothesized remodeling should involve other proteins that are components of the incision system but that are also required for TCR, making TFIIH and XPG prime candidates.

We used a minimalist in vitro system to ask whether RNAPII blocks incision by XPG and whether TFIIH affects the block. Purified RNAPIIa alone binds to a 15 nt DNA bubble as established by EMSA (Figure 5C, lane 1). This substrate is not the optimal size (~30 nt) for incision by XPG but resembles the size of transcription bubbles. Using reaction conditions in which XPG efficiently incised the labeled bubble (Figure 5A, lane 2), we found that prior addition of RNAPII blocked incision by approximately 90% (compare lanes 2 and 3), presumably through steric hindrance. Incision reaction samples were divided, and one portion of each was analyzed by EMSA to detect protein binding to the DNA substrate (Figure 5B). The position of the XPG/RNAPII supershifted complex from the incision reaction is indicated by comparison to the complex formed under standard binding conditions (Figures 5B and 5C). The large fraction of RNAPII complexed with XPG on the bubble in the latter case suggests that XPG interacts preferentially with bubbles to which RNAPII is bound (Figure 5C, lane 3) compared to the DNA bubble itself (lane 2).

Because TFIIH is required for TCR in an unknown capacity, we next asked whether it had any effect on incision. Addition of TFIIH alone had only a slight effect on the inhibition of incision by bound RNAPII (Figures 5A and 5D, lane 4 in each), but strikingly, addition of ATP along with TFIIH substantially relieved the inhibition, allowing approximately 50% of the incisions made by XPG alone (Figures 5A and 5D, lane 5 in each). A control reaction showed no significant effect of TFIIH plus ATP on incision in the absence of RNAPII (Figures 5A and 5D, lane 8 in each). Importantly, the restoration of incision was not accompanied by the release of bound RNAPII, although the polymerase evidently became hyperphosphorylated as judged by decreased mobility

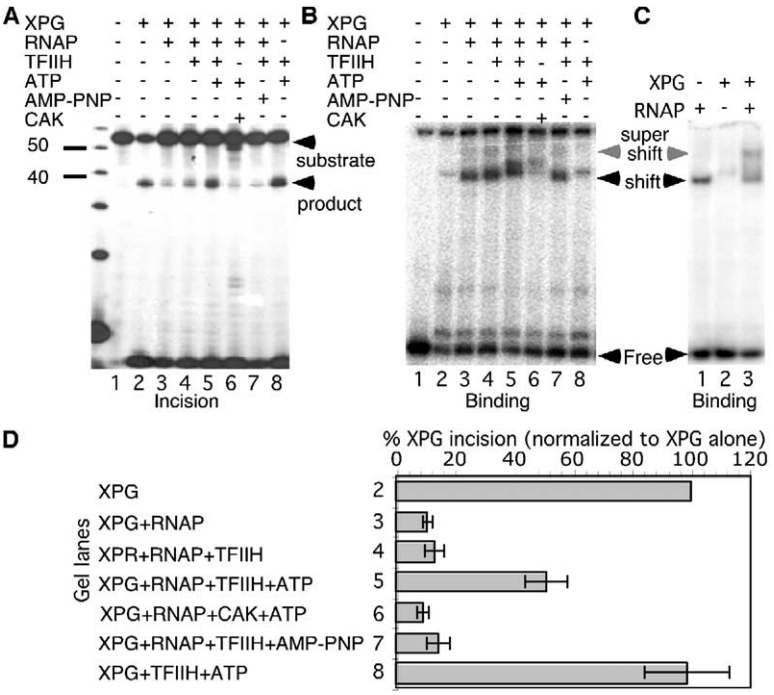

Figure 5. TFIIH and ATP Relieve Inhibition of XPG Incision by Bound RNAPII

XPG (33 nM) was incubated with 6.6 nM labeled 15 nt DNA bubble substrate. Where indicated, 18.5 nM RNAPIIa was preincubated with the DNA for 5 min before addition of XPG with or without 0.93 pmol TFIIH, 1.5 mM ATP or AMP-PNP, or 100 ng of CAK kinase in 20 μl under standard incision reaction conditions but with 2 mM $MgCl_2$. The samples were incubated at 37°C for 2 hr and split for analysis of both incision and binding.

(A) Denaturing gel separating incision product from substrate. There was a significant 5′ nuclease activity in the XPG preparation as observed previously (Evans et al., 1997a).

(B) EMSA of incision reactions showing retention of RNAPII binding to substrate. Half of each reaction run on the denaturing gel in (A) was run on a native gel.

(C) EMSA showing relative mobility of 17 nM XPG and/or 18.5 nM RNAPII complexes with 15 nt bubble DNA and formation of supracomplex. Binding was under standard EMSA conditions in the absence of $MgCl_2$.

(D) The amount of incision product relative to total DNA was determined for each reaction condition and normalized to incision by XPG alone. Average values from three incision experiments including the gel in (A) are shown. Error bars indicate standard deviation of the mean.

of the complex (Figure 5B, compare lane 5 to lane 4). Hydrolysis of ATP is required, because addition of the nonhydrolyzable analog AMP-PNP had no effect either on incision or on the mobility of the complex (Figures 5A, 5B, and 5D, lane 7 in each). There are two separate activities of TFIIH known to involve ATP hydrolysis: phosphorylation of the C-terminal domain of RNAPII by the cdk7 component of the CAK subunit to initiate transcription (Tirode et al., 1999) and the helicase activities of XPB and XPD. Because the position of the incision did not change in the presence of TFIIH (Figure 5A), it is unlikely that its DNA helicase activities are involved. We therefore asked whether addition of the CAK subunit alone could similarly relieve inhibition of XPG incision activity. However, CAK in the presence of ATP actually led to a slight further decrease in incision by XPG (Figures 5A and 5D, lane 6 in each), despite apparently phosphorylating bound RNAPII, as indicated by decreased mobility (Figure 5B, lane 6). These results suggest that RNAPII bound to bubble DNA can be remodeled by TFIIH in an ATP hydrolysis-dependent process to give XPG access to the bubble junction for incision, supporting the possibility that RNAPII can remain bound to the DNA at the lesion during TCR and suggesting a new function for TFIIH in TCR.

Discussion

To date, no clear molecular explanation has been provided for the postnatal requirement for noncatalytic functions of XPG. Furthermore, the mechanism by which the TCR machinery recognizes transcription complexes stalled by DNA damage and initiates the rapid preferential removal of transcription-blocking lesions has remained mysterious. To address these issues, we have characterized functionally important interactions of XPG with DNA and with CSB, TFIIH, and RNAPII. Our results implicate the R-domain and C-terminal domain of XPG in noncatalytic functions of XPG involving the recognition of stalled RNAPII and the stimulation of CSB activity, predict the importance of these domains for normal postnatal development and viability, and suggest a model for early events in TCR that invokes a requirement for XPG and a conformational change in stalled RNAPII that is induced by TFIIH.

Remodeling of Stalled RNAPII and Implications for TCR

The results of Figure 5 are consistent with the interpretation that TFIIH utilizes ATP hydrolysis to alter the conformation of RNAPII bound to a transcription-sized DNA bubble, such that the otherwise inaccessible bubble junction becomes available for incision by XPG. This surprising result provides an explanation for two previous reports that excision of transcription-blocking lesions could occur despite the presence of the stalled RNAPII (Selby et al., 1997; Tremeau-Bravard et al., 2004). It implies that the repair steps of TCR may proceed without removal of the arrested polymerase and suggests that the function of TFIIH in TCR may be remodeling of RNAPII. Structural studies of yeast RNAPII provide insight into how this might be achieved. The clamp module of the polymerase is highly mobile, and in the conversion from initiation to elongation mode it rotates 30 degrees to trap the template and growing transcript (Gnatt et al., 2001). Our results suggest that

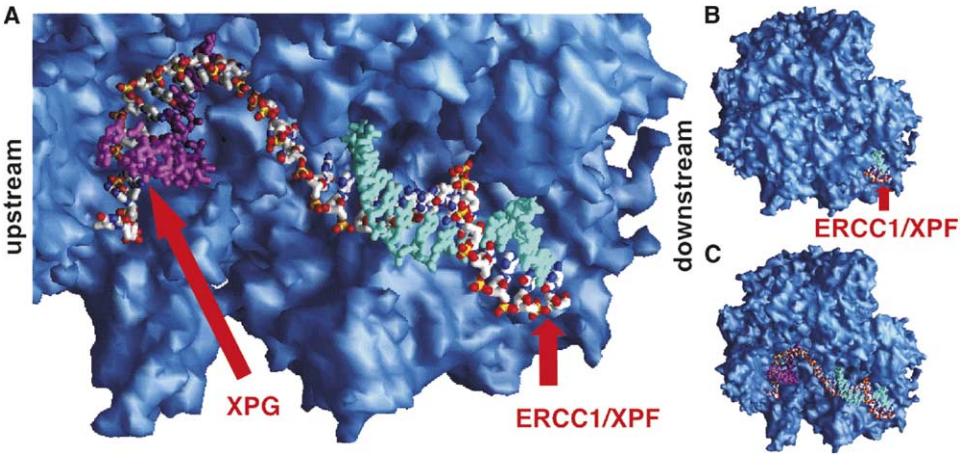

Figure 6. Structural Models of Stalled RNAPII

(A) Close-up view of a surface model of the yeast RNAPII crystal structure, showing the relative positions of the downstream duplex DNA and the template strand and RNA/DNA hybrid portions of the transcription bubble with the clamp module removed to reveal them. The RNA/DNA is depicted as a stick model, with the RNA colored in magenta, the NTS colored in cyan, and the TS colored according to atom type (carbon, phosphorus, oxygen, and nitrogen colored in white, yellow, red, and blue, respectively). The positions of XPG and ERCC1/XPF incision sites relative to a hypothetical lesion located at the polymerase active site are indicated by arrows. The model was based on 1R9T pdb coordinates (Westover et al., 2004) and made using the GRASP program (Nicholls et al., 1991).

(B) Surface model of the entire yeast RNAPII. An identical perspective as in (A) is shown but with the clamp module in place, showing that the transcription bubble is enclosed within the polymerase in its elongating form.

(C) Identical view as in (B), with the clamp module removed as in (A).

TFIIH may be able to reverse this rotation of the clamp domain to allow access of repair proteins during TCR. The inferred RNAPII remodeling is ATP hydrolysis-dependent but must require a function of TFIIH other than (or in addition to) phosphorylation of the CTD, as the CAK subunit alone did not allow incision despite hyperphosphorylating RNAPII. It thus may either involve phosphorylation events specific to the holocomplex or require interaction with other components of TFIIH.

The footprint of RNAPII stalled at a lesion is ~35 nt, significantly larger than the 14–22 nt transcription bubble, and is positioned asymmetrically with respect to the lesion (Tornaletti et al., 1999). The crystal structure of a ternary complex of yeast RNAPII has revealed the positions of the downstream duplex and the RNA/DNA hybrid regions in the complex (Westover et al., 2004; Figures 6A–6C). However, neither the NTS of the bubble nor the upstream duplex region was visible in the electron density, with the crystallographic disorder suggesting that these regions were not tightly bound by the polymerase. The implied relative accessibility of the NTS would be consistent with its requirement for formation of XPG and CSB complexes with stalled RNAPII (Figure 1G).

Assuming that RNAPII arrests with the lesion either in the polymerization site or in the –1 position, the site of XPG incision in TCR as predicted from studies of reconstituted NER (Evans et al., 1997b) would be at or near the upstream junction of the transcription bubble (left arrow in Figure 6A). This junction is clearly not accessible with the clamp module in the closed position, but the proposed conformational change is predicted to allow access to it (Figures 6A–6C). In our minimalist model system, XPG incises the 3′ strand on either side of an unobstructed bubble but only incision of the labeled strand is detected. However, the orientation of RNAPII on the bubble should be random, so remodeling affecting only one junction should lead to an ~50% restoration of incision, as was in fact observed (Figure 5D). Thus, it is possible that the downstream junction of the bubble is not exposed by the proposed remodeling. In contrast to the XPG incision site, the predicted position of the 5′ incision by ERCC1/XPF in TCR would not be at a transcription bubble junction but rather in the downstream duplex region not covered by RNAPII (arrows in Figures 6A and 6B), so access to it should not be affected by the stalled polymerase. However, in the repair stage of TCR, further unwinding of the transcription bubble downstream of the lesion would be required for the 5′ incision, presumably by TFIIH after recruitment of XPA and RPA.

Implication of Noncatalytic Domains of XPG in TCR and CS

The preferential binding of transcription-sized DNA bubbles by XPG and the separation of DNA bubble binding from incision activity (Figures 2 and 3) are presumably relevant to the function of XPG in TCR. That the R- and C-terminal domains of XPG are essential for DNA bubble binding, but not for incision, implies that these domains should be essential for the TCR function of XPG and implicated in CS. In agreement with this notion, the functional interaction of XPG with CSB was mapped to the C-terminal domain (Figures 4D and 4E). Notably, patient mutations in *XPG* that give rise to early infantile CS all involve severe truncations of the protein that would eliminate either the C-terminal domain or

both R- and C-terminal domains (Emmert et al., 2002; Nouspikel et al., 1997). Moreover, *xpg* mutant mice in which the C-terminal domain, encoded by exon 15, is deleted suffer severe postnatal growth retardation and very early death (the mouse version of the CS phenotype), although this phenotype is not revealed unless *XPA* is also deleted (Shiomi et al., 2005). The requirement for loss of XPA, which alone does not result in any developmental defects, may reflect overlapping functions of NER and TCR in responses to endogenous lesions and thus an increased burden on TCR when NER is inactivated (Andressoo and Hoeijmakers, 2005). In any case, the result emphasizes the importance of the C-terminal domain of XPG in nonenzymatic functions that are critical for postnatal development and viability. Our results would predict that the R-domain of XPG should similarly be essential for TCR. Interestingly, an unusual XP-G/CS patient with late onset of CS symptoms and an uncharacteristically long life span (>28 years) harbored a homozygous mutation leading to an alternatively spliced, near full-length gene product but with a deletion of 7 amino acids in the R-domain (Thorel et al., 2004). The delayed CS phenotype in this patient cannot be explained by loss of NER, because neither XP-A patients nor XP-G patients with missense mutations lacking NER exhibit CS symptoms (Emmert et al., 2002; Lalle et al., 2002; Nouspikel et al., 1997). Instead, it is consistent with a subtle defect in the noncatalytic TCR function of XPG and a requirement for the R-domain in that function. The fact that deletion of the R-domain or portions of it also interferes with NER (Dunand-Sauthier et al., 2005; Thorel et al., 2004) predicts that mice lacking the XPG R-domain should exhibit the CS phenotype in the absence of any other mutations.

Model for TCR and Insights for Cockayne Syndrome

Our results provide insights into the mechanism of TCR and suggest functions in it for XPG and TFIIH. We propose a mechanism involving joint recognition of stalled RNAPII by XPG and CSB as the initiating step in TCR (Figure 7). A second critical function of CSB is recruitment of TFIIH, as suggested both by in vitro (Tantin, 1998) and in vivo (Tijsterman et al., 1997; Tu et al., 1997) studies. Because TFIIH does not recognize stalled RNAPII ternary complexes on its own (Tantin, 1998), but XPG does (Figure 1), and XPG interacts stably with TFIIH in the cell (Araujo et al., 2001), the finding that TFIIH is able to remodel RNAPII bound to bubble DNA without CSB but in the presence of XPG (Figure 5) suggests that XPG may also recruit TFIIH. Thus, CSB and XPG may have overlapping or cooperative functions in TFIIH recruitment during TCR as well as in recognition of the RNAPII. Another function of CSB in TCR may be related to its ATPase-dependent ability to remodel histones (Citterio et al., 2000) and/or other DNA bound proteins. Our observation of bubble-dependent stimulation of CSB ATPase activity by XPG (Figure 4) suggests that this function also would likely be cooperative. Because XPG provides a clear enhancement of multiple CSB functions, in cells lacking XPG the function of CSB may also be impaired. CSA is also rigorously required for TCR, and its recruitment has been shown to depend on CSB (Kamiuchi et al., 2002), but

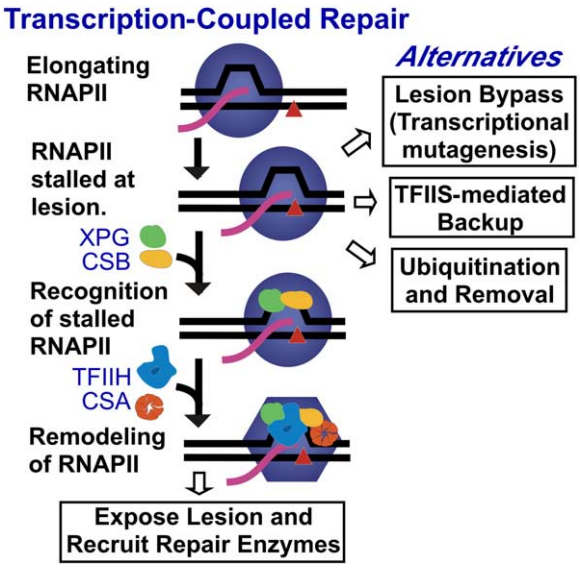

Figure 7. Model for Early Steps in TCR and Alternative Processes

Elongating RNAPII is stalled at a lesion (red triangle). XPG and CSB cooperatively recognize and interact with the stalled RNAPII. TFIIH and CSA are subsequently recruited by XPG and CSB acting cooperatively. TFIIH remodels RNAPII, opening the clamp domain to expose the lesion, thus allowing access of XPG to the transcription bubble. Recruitment of XPA, RPA, and ERCC1/XPF allows excision of the lesion without removal of RNAPII. Transcriptional bypass of the lesion, backup by TFIIS, or RNAPII degradation may represent alternatives to TCR as a means to resolve stalled transcription.

the exact function of CSA and the possible involvement of XPG remain to be determined.

Our results suggest that in contrast to most accepted models for TCR, removal of the stalled RNAPII may not be necessary to allow repair (Figure 7). We propose that TFIIH induces a phosphorylation-dependent conformational change in the polymerase through reversal of the locking down of its clamp module, thus allowing access of XPG to the upstream junction of the transcription bubble. The inferred remodeling of RNAPII observed in our minimalist model system is independent of CSB, any damage-induced modifications, or indeed of a lesion. The lack of a requirement for CSB in the remodeling is in keeping with observations from partially purified or reconstituted systems (Selby et al., 1997; Tremeau-Bravard et al., 2004). However, events at a stalled transcription complex in the cell and in the context of chromatin are obviously much more complex, and roles for CSB, CSA, and/or damage-induced modifications of RNAPII in the remodeling are clearly possible. Subsequent recruitment of the remaining complement of proteins necessary for the excision step of TCR of bulky lesions (XPA, RPA, ERCC1/XPF) is proposed to allow excision of the lesion without removal of RNAPII. Evidence from in vitro studies (Selby et al., 1997; Tremeau-Bravard et al., 2004) suggests that the repair-synthesis step can also be completed in the presence of the RNAPII, although how this would be achieved is not clear.

There are likely to be multiple alternative processes for resolution of stalled RNAPII (Svejstrup, 2003) (Figure

7), with TCR being the pathway of choice perhaps because, as suggested by our results, it allows repair without disruption of the transcription complex. An alternative to TCR may be bypass of the lesion by RNAPII, with elevated probability of errors in insertion opposite the lesion ("transcriptional mutagenesis"), as has been demonstrated in bacteria (Bregeon et al., 2003). Whether these two pathways are completely independent or may involve some common event such as remodeling of RNAPII remains to be determined. Yet another possibility is backup of RNAPII mediated by the transcription elongation factor TFIIS (Tornaletti et al., 1999). However, CSB actually appears to prevent TFIIS action (Selby and Sancar, 1997; Tremeau-Bravard et al., 2004), and backup of RNAPII is more likely an alternative to TCR rather than part of the TCR mechanism, perhaps serving to allow another chance for global NER to access the lesion. Finally, if TCR fails, ubiquitin-mediated degradation of arrested RNAPII by the proteasome may be a last resort (Woudstra et al., 2002).

Our finding that XPG and CSB recognize RNAPII stalled by nucleotide deprivation suggests that TCR proteins may also help to resolve transcription through nonlesion impediments to elongation, thus effectively serving as elongation factors as proposed for CSB (Yu et al., 2000). This interpretation could explain the observation that the yeast homologs of CSB and XPG are involved in maintaining high levels of transcription in the absence of extrinsic damage (Lee et al., 2001, 2002).

Taken together, the molecular associations and DNA bubble binding preferences of XPG support its role with CSB in coordinated recognition of stalled transcription to initiate TCR and promote TFIIH-dependent remodeling of stalled RNAPII. Our results suggest new functions for XPG and TFIIH in TCR, provide a molecular explanation for the postnatal developmental failure and mortality caused by loss of XPG, and identify the noncatalytic R- and C-terminal domains of XPG as likely to be critical in this regard, in agreement with mouse models and patient mutations in XP-G/CS.

Experimental Procedures

Nucleotide Substrates

Sequences of DNA and RNA substrates are shown in Figure S1. For intrastrand crosslink formation, the TS in the cis-Pt substrate contained a unique GTG sequence coincident with an ApaL1 restriction site. It was incubated 1:12 with cisplatin at 37°C for 24 hr in the dark and modification was confirmed by resistance to digestion and mobility change in denaturing polyacrylamide gel electrophoresis (PAGE) (Shivji et al., 1999). Bubble substrates were formed from two oligos with a central noncomplementary region (polyT opposite polyC) of varying length flanked by 20 nt dsDNA arms. For DNA binding and incision assays, the 5′ ends of the T-containing strands were labeled with γ-^{32}P-ATP by polynucleotide kinase (Promega).

Antibodies

Two antibodies against the R-domain of XPG were generated by immunizing rabbits with either cyclized R1 or R2 peptide (acetylated-CC^{181}HNPQAIDIESEDFSSLPPEVKHE^{203}C-amide or acetylated-C^{267}EDEGGFLKEVESRRV^{281}CC-amide, respectively). Peptides were reduced with 12 mM DTT, purified on a G10 Sephadex column (GE Healthcare), and conjugated to KLH prior to immunization. Polyclonal peptide antibodies were affinity purified from sera by using an amide-linked peptide column (GE Healthcare). The XPG mouse monoclonal antibody 8H7 was from Novus or Neomarkers; its epitope maps to residues between Ser947 and Ala1165 (Novus Biologicals, personal communication). Other antibodies were commercial: HA (Boehringer Mannheim, 12CA5); TFIIH p89 (Santa Cruz Biotechnology, sc293); RNAPII (Santa Cruz Biotechnology, sc899); RNAPIIo (H5, Covance); and Tetra-His (Qiagen).

Expression and Purification of Proteins

Details of the expression and purification of proteins are in the Supplemental Data. Full-length XPG was expressed recombinantly in insect cells and purified as described (Evans et al., 1997a). To generate the XFX construct, residues 79–785 were replaced with residues 82–128 from *P. furiosus* FEN-1 (Hosfield et al., 1998). XPGΔC contains the first 1012 amino acids of XPG, terminating just after the conserved PCNA binding domain. XFXΔC is similar to XFX but has the C-terminal truncation of XPGΔC. The GST fusion C-terminal construct begins at residue 1012 and was bacterially expressed. R-domain (residues 86–765) was also bacterially expressed. CSB with an N-terminal His tag and a C-terminal HA tag was expressed in insect cells and purified as described (Citterio et al., 1998). Specific activity of different preparations varied. Native human RNAPII and TFIIH were purified from HeLa cell nuclei as described (LeRoy et al., 1998; Maldonado et al., 1996). Recombinant human RPA from *E. coli* was the generous gift of Sam Bennett and Dale Mosbaugh. The CAK subunit of TFIIH was from Upstate; BSA was from Sigma.

Protein-Protein Interaction Assays

Details of coimmunoprecipitation and Far Western blotting assays are in the Supplemental Data. For XPG and RNAPII coimmunoprecipitation from HeLa cells, nuclei from 2.3 liters of HeLa cells were prepared as described (Maldonado et al., 1996).

In Vitro Transcription by RNAPII and Complex Formation

A promoterless RNAPII initiation complex was prepared by using purified human RNAPII as described (Sidorenkov et al., 1998). For elongation, the initiation complex was incubated for 30 min as previously described except with 150 μg BSA, 10 U RNase inhibitor, and no PMSF (Tantin et al., 1997). Then, it was incubated for 15 min with CSB (148 nM) and/or XPG (223 nM) and loaded onto a 4% native PAGE gel containing 1% glycerol and 2 mM $MgCl_2$. Electrophoresis was at 4°C. Gels were visualized by autoradiography. Studies that involved stalling of the RNAPII by nucleotide deprivation were as above, except that 134 nM CSB, 150 nM XPG, 250 μM each of GTP and ATP, 10 μM CTP, and 4 μCi [α-^{32}P]CTP were used. Exact amounts of RNAPII involved in elongation were not determined.

DNA Binding by EMSA

Labeled DNA substrates (5 nM) were incubated for 20 min at RT in a 20 μl reaction containing 10 mM HEPES (pH 7.5), 110 mM KCl, 1 mM EDTA, 1 mM DTT, 4% glycerol, and 0.2 μg poly(dI:dC). Separation was on a 4.5% native PAGE gel in 0.5× TBE buffer. Quantification was with ImageQuant (Molecular Dynamics).

DNA Bubble Incision Assays

The XPG incision assay was slightly modified from (Evans et al., 1997a). Briefly, 0.5–2 nM XPG protein was incubated with ^{32}P-labeled DNA substrate (2.5 nM) at 37°C in 25 mM HEPES (pH 7.5), 1% glycerol, 1 mM DTT, 0.25 mg/ml BSA, and 4 mM $MgCl_2$. Protein and substrate concentrations for the incision experiments of Figure 5 were different (see legend).

CSB ATPase Assays

ATPase assays were performed as described (Citterio et al., 1998) with 10 nt bubble or linear DNA (57-mer) using 1.125 pmol of DNA per reaction, 5 nM CSB, and/or 5 nM XPG. For assays with XPG domain constructs, 120 nM CSB, 60 nM XPG, 120 nM GST-C-term, 120 nM XFXΔC, or 80 nM RPA was used. Substrate and product were separated by thin-layer chromatography and quantified by phosphorimager.

Supplemental Data

Supplemental Data including four figures, Supplemental Experimental Procedures, and Supplemental References are available online with this article at http://www.molecule.org/cgi/content/full/20/2/187/DC1/.

Acknowledgments

We thank Stuart Clarkson for *XPG* cDNA and Jan Hoeijmakers for the CSB expression construct. Purified recombinant RPA was a generous gift from Sam Bennett and Dale Mosbaugh. We thank J. Perry for R2 antibody purification; J. Fang for HeLa cell production and harvest; Ely Kwoh for phosphorimager quantification; C. Kane for helpful discussions; and J. Fuss and B. Haltiwanger for comments on the manuscript. These studies were supported by the National Institutes of Health (NIH) Structural Cell Biology of DNA Repair Machines P01 grant CA92584 (J.A.T., P.K.C., E.N.), by NIH grants CA63503 (P.K.C.) and GM63072 (E.N.), by a Canadian Institutes of Health Research postdoctoral fellowship to E.C., and by the Office of Science, Office of Biological and Environmental Research, U.S. Department of Energy, under Contract Number DE-AC02-05CH11231.

Received: April 20, 2005
Revised: August 8, 2005
Accepted: September 30, 2005
Published: October 27, 2005

References

Andressoo, J.O., and Hoeijmakers, J.H. (2005). Transcription-coupled repair and premature ageing. Mutat. Res. *577*, 179–194.

Araujo, S.J., Nigg, E.A., and Wood, R.D. (2001). Strong functional interactions of TFIIH with XPC and XPG in human DNA nucleotide excision repair, without a preassembled repairosome. Mol. Cell. Biol. *21*, 2281–2291.

Berneburg, M., and Lehmann, A.R. (2001). Xeroderma pigmentosum and related disorders: defects in DNA repair and transcription. Adv. Genet. *43*, 71–102.

Bradsher, J., Auriol, J., Proietti de Santis, L., Iben, S., Vonesch, J.L., Grummt, I., and Egly, J.M. (2002). CSB is a component of RNA pol I transcription. Mol. Cell *10*, 819–829.

Bregeon, D., Doddridge, Z.A., You, H.J., Weiss, B., and Doetsch, P.W. (2003). Transcriptional mutagenesis induced by uracil and 8-oxoguanine in Escherichia coli. Mol. Cell *12*, 959–970.

Christiansen, M., Stevnsner, T., Modin, C., Martensen, P.M., Brosh, R.M., Jr., and Bohr, V.A. (2003). Functional consequences of mutations in the conserved SF2 motifs and post-translational phosphorylation of the CSB protein. Nucleic Acids Res. *31*, 963–973.

Citterio, E., Rademakers, S., van der Horst, G.T., van Gool, A.J., Hoeijmakers, J.H., and Vermeulen, W. (1998). Biochemical and biological characterization of wild-type and ATPase-deficient Cockayne syndrome B repair protein. J. Biol. Chem. *273*, 11844–11851.

Citterio, E., Van Den Boom, V., Schnitzler, G., Kanaar, R., Bonte, E., Kingston, R.E., Hoeijmakers, J.H., and Vermeulen, W. (2000). ATP-dependent chromatin remodeling by the Cockayne syndrome B DNA repair-transcription-coupling factor. Mol. Cell. Biol. *20*, 7643–7653.

Coin, F., and Egly, J.M. (1998). Ten years of TFIIH. Cold Spring Harb. Symp. Quant. Biol. *63*, 105–110.

Constantinou, A., Gunz, D., Evans, E., Lalle, P., Bates, P.A., Wood, R.D., and Clarkson, S.G. (1999). Conserved residues of human XPG protein important for nuclease activity and function in nucleotide excision repair. J. Biol. Chem. *274*, 5637–5648.

Donahue, B.A., Yin, S., Taylor, J.S., Reines, D., and Hanawalt, P.C. (1994). Transcript cleavage by RNA polymerase II arrested by a cyclobutane pyrimidine dimer in the DNA template. Proc. Natl. Acad. Sci. USA *91*, 8502–8506.

Dunand-Sauthier, I., Hohl, M., Thorel, F., Jaquier-Gubler, P., Clarkson, S.G., and Scharer, O.D. (2005). The spacer region of XPG mediates recruitment to nucleotide excision repair complexes and determines substrate specificity. J. Biol. Chem. *280*, 7030–7037.

Emmert, S., Slor, H., Busch, D.B., Batko, S., Albert, R.B., Coleman, D., Khan, S.G., Abu-Libdeh, B., DiGiovanna, J.J., Cunningham, B.B., et al. (2002). Relationship of neurologic degeneration to genotype in three xeroderma pigmentosum group G patients. J. Invest. Dermatol. *118*, 972–982.

Evans, E., Fellows, J., Coffer, A., and Wood, R.D. (1997a). Open complex formation around a lesion during nucleotide excision repair provides a structure for cleavage by human XPG protein. EMBO J. *16*, 625–638.

Evans, E., Moggs, J.G., Hwang, J.R., Egly, J.M., and Wood, R.D. (1997b). Mechanism of open complex and dual incision formation by human nucleotide excision repair factors. EMBO J. *16*, 6559–6573.

Fiedler, U., and Timmers, H.T. (2001). Analysis of the open region of RNA polymerase II transcription complexes in the early phase of elongation. Nucleic Acids Res. *29*, 2706–2714.

Gnatt, A.L., Cramer, P., Fu, J., Bushnell, D.A., and Kornberg, R.D. (2001). Structural basis of transcription: an RNA polymerase II elongation complex at 3.3 A resolution. Science *292*, 1876–1882.

Harada, Y.N., Shiomi, N., Koike, M., Ikawa, M., Okabe, M., Hirota, S., Kitamura, Y., Kitagawa, M., Matsunaga, T., Nikaido, O., and Shiomi, T. (1999). Postnatal growth failure, short life span, and early onset of cellular senescence and subsequent immortalization in mice lacking the xeroderma pigmentosum group G gene. Mol. Cell. Biol. *19*, 2366–2372.

Harrington, J.J., and Lieber, M.R. (1994). Functional domains within FEN-1 and RAD2 define a family of structure-specific endonucleases: implications for nucleotide excision repair. Genes Dev. *8*, 1344–1355.

Hoeijmakers, J.H. (2001). Genome maintenance mechanisms for preventing cancer. Nature *411*, 366–374.

Hohl, M., Thorel, F., Clarkson, S.G., and Scharer, O.D. (2003). Structural determinants for substrate binding and catalysis by the structure-specific endonuclease XPG. J. Biol. Chem. *278*, 19500–19508.

Hosfield, D.J., Mol, C.D., Shen, B., and Tainer, J.A. (1998). Structure of the DNA repair and replication endonuclease and exonuclease FEN-1: coupling DNA and PCNA binding to FEN-1 activity. Cell *95*, 135–146.

Iyer, N., Reagan, M.S., Wu, K.J., Canagarajah, B., and Friedberg, E.C. (1996). Interactions involving the human RNA polymerase II transcription/nucleotide excision repair complex TFIIH, the nucleotide excision repair protein XPG, and Cockayne syndrome group B (CSB) protein. Biochemistry *35*, 2157–2167.

Kamiuchi, S., Saijo, M., Citterio, E., de Jager, M., Hoeijmakers, J.H., and Tanaka, K. (2002). Translocation of Cockayne syndrome group A protein to the nuclear matrix: possible relevance to transcription-coupled DNA repair. Proc. Natl. Acad. Sci. USA *99*, 201–206.

Kireeva, M.L., Komissarova, N., and Kashlev, M. (2000). Overextended RNA:DNA hybrid as a negative regulator of RNA polymerase II processivity. J. Mol. Biol. *299*, 325–335.

Lalle, P., Nouspikel, T., Constantinou, A., Thorel, F., and Clarkson, S.G. (2002). The founding members of xeroderma pigmentosum group G produce XPG protein with severely impaired endonuclease activity. J. Invest. Dermatol. *118*, 344–351.

Laybourn, P.J., and Dahmus, M.E. (1990). Phosphorylation of RNA polymerase IIA occurs subsequent to interaction with the promoter and before the initiation of transcription. J. Biol. Chem. *265*, 13165–13173.

Lee, S.K., Yu, S.L., Prakash, L., and Prakash, S. (2001). Requirement for yeast RAD26, a homolog of the human CSB gene, in elongation by RNA polymerase II. Mol. Cell. Biol. *21*, 8651–8656.

Lee, S.K., Yu, S.L., Prakash, L., and Prakash, S. (2002). Requirement of yeast RAD2, a homolog of human XPG gene, for efficient RNA polymerase II transcription. implications for Cockayne syndrome. Cell *109*, 823–834.

Lehmann, A.R. (2001). The xeroderma pigmentosum group D (XPD)

gene: one gene, two functions, three diseases. Genes Dev. *15*, 15–23.

Lehmann, A.R. (2003). DNA repair-deficient diseases, xeroderma pigmentosum, Cockayne syndrome and trichothiodystrophy. Biochimie *85*, 1101–1111.

LeRoy, G., Drapkin, R., Weis, L., and Reinberg, D. (1998). Immunoaffinity purification of the human multisubunit transcription factor IIH. J. Biol. Chem. *273*, 7134–7140.

Ljungman, M., and Lane, D.P. (2004). Transcription—guarding the genome by sensing DNA damage. Nat. Rev. Cancer *4*, 727–737.

Maldonado, E., Drapkin, R., and Reinberg, D. (1996). Purification of human RNA polymerase II and general transcription factors. Methods Enzymol. *274*, 72–100.

Mayne, L.V., and Lehmann, A.R. (1982). Failure of RNA synthesis to recover after UV irradiation. An early defect in cells from individuals with Cockayne's syndrome and xeroderma pigmentosum. Cancer Res. *42*, 1473–1478.

Mellon, I., Spivak, G., and Hanawalt, P.C. (1987). Selective removal of transcription-blocking DNA damage from the transcribed strand of the mammalian DHFR gene. Cell *51*, 241–249.

Nicholls, A., Sharp, K.A., and Honig, B. (1991). Protein folding and association: insights from the interfacial and thermodynamic properties of hydrocarbons. Proteins *11*, 281–296.

Nouspikel, T., Lalle, P., Leadon, S.A., Cooper, P.K., and Clarkson, S.G. (1997). A common mutational pattern in Cockayne syndrome patients from xeroderma pigmentosum group G: implications for a second XPG function. Proc. Natl. Acad. Sci. USA *94*, 3116–3121.

Rapin, I., Lindenbaum, Y., Dickson, D.W., Kraemer, K.H., and Robbins, J.H. (2000). Cockayne syndrome and xeroderma pigmentosum. Neurology *55*, 1442–1449.

Selby, C.P., and Sancar, A. (1997). Cockayne syndrome group B protein enhances elongation by RNA polymerase II. Proc. Natl. Acad. Sci. USA *94*, 11205–11209.

Selby, C.P., Drapkin, R., Reinberg, D., and Sancar, A. (1997). RNA polymerase II stalled at a thymine dimer: footprint and effect on excision repair. Nucleic Acids Res. *25*, 787–793.

Selzer, R.R., Nyaga, S., Tuo, J., May, A., Muftuoglu, M., Christiansen, M., Citterio, E., Brosh, R.M., Jr., and Bohr, V.A. (2002). Differential requirement for the ATPase domain of the Cockayne syndrome group B gene in the processing of UV-induced DNA damage and 8-oxoguanine lesions in human cells. Nucleic Acids Res. *30*, 782–793.

Shiomi, N., Kito, S., Oyama, M., Matsunaga, T., Harada, Y.N., Ikawa, M., Okabe, M., and Shiomi, T. (2004). Identification of the XPG region that causes the onset of Cockayne syndrome by using Xpg mutant mice generated by the cDNA-mediated knock-in method. Mol. Cell. Biol. *24*, 3712–3719.

Shiomi, N., Mori, M., Kito, S., Harada, Y.N., Tanaka, K., and Shiomi, T. (2005). Severe growth retardation and short life span of double-mutant mice lacking Xpa and exon 15 of Xpg. DNA Repair (Amst.) *4*, 351–357.

Shivji, M.K., Moggs, J.G., Kuraoka, I., and Wood, R.D. (1999). Dual-incision assays for nucleotide excision repair using DNA with a lesion at a specific site. Methods Mol. Biol. *113*, 373–392.

Sidorenkov, I., Komissarova, N., and Kashlev, M. (1998). Crucial role of the RNA:DNA hybrid in the processivity of transcription. Mol. Cell *2*, 55–64.

Svejstrup, J.Q. (2002). Mechanisms of transcription-coupled DNA repair. Nat. Rev. Mol. Cell Biol. *3*, 21–29.

Svejstrup, J.Q. (2003). Rescue of arrested RNA polymerase II complexes. J. Cell Sci. *116*, 447–451.

Tantin, D. (1998). RNA polymerase II elongation complexes containing the Cockayne syndrome group B protein interact with a molecular complex containing the transcription factor IIH components xeroderma pigmentosum B and p62. J. Biol. Chem. *273*, 27794–27799.

Tantin, D., Kansal, A., and Carey, M. (1997). Recruitment of the putative transcription-repair coupling factor CSB/ERCC6 to RNA polymerase II elongation complexes. Mol. Cell. Biol. *17*, 6803–6814.

Thorel, F., Constantinou, A., Dunand-Sauthier, I., Nouspikel, T., Lalle, P., Raams, A., Jaspers, N.G., Vermeulen, W., Shivji, M.K., Wood, R.D., and Clarkson, S.G. (2004). Definition of a short region of XPG necessary for TFIIH interaction and stable recruitment to sites of UV damage. Mol. Cell. Biol. *24*, 10670–10680.

Tian, M., Jones, D.A., Smith, M., Shinkura, R., and Alt, F.W. (2004). Deficiency in the nuclease activity of xeroderma pigmentosum G in mice leads to hypersensitivity to UV irradiation. Mol. Cell. Biol. *24*, 2237–2242.

Tijsterman, M., Verhage, R.A., van de Putte, P., Tasseron-de Jong, J.G., and Brouwer, J. (1997). Transitions in the coupling of transcription and nucleotide excision repair within RNA polymerase II-transcribed genes of Saccharomyces cerevisiae. Proc. Natl. Acad. Sci. USA *94*, 8027–8032.

Tirode, F., Busso, D., Coin, F., and Egly, J.M. (1999). Reconstitution of the transcription factor TFIIH: assignment of functions for the three enzymatic subunits, XPB, XPD, and cdk7. Mol. Cell *3*, 87–95.

Tornaletti, S., and Hanawalt, P.C. (1999). Effect of DNA lesions on transcription elongation. Biochimie *81*, 139–146.

Tornaletti, S., Reines, D., and Hanawalt, P.C. (1999). Structural characterization of RNA polymerase II complexes arrested by a cyclobutane pyrimidine dimer in the transcribed strand of template DNA. J. Biol. Chem. *274*, 24124–24130.

Tremeau-Bravard, A., Riedl, T., Egly, J.M., and Dahmus, M.E. (2004). Fate of RNA polymerase II stalled at a cisplatin lesion. J. Biol. Chem. *279*, 7751–7759.

Tu, Y., Bates, S., and Pfeifer, G.P. (1997). Sequence-specific and domain-specific DNA repair in xeroderma pigmentosum and Cockayne syndrome cells. J. Biol. Chem. *272*, 20747–20755.

van Gool, A.J., Citterio, E., Rademakers, S., van Os, R., Vermeulen, W., Constantinou, A., Egly, J.M., Bootsma, D., and Hoeijmakers, J.H. (1997). The Cockayne syndrome B protein, involved in transcription-coupled DNA repair, resides in an RNA polymerase II-containing complex. EMBO J. *16*, 5955–5965.

van Hoffen, A., Natarajan, A.T., Mayne, L.V., van Zeeland, A.A., Mullenders, L.H., and Venema, J. (1993). Deficient repair of the transcribed strand of active genes in Cockayne's syndrome cells. Nucleic Acids Res. *21*, 5890–5895.

Westover, K.D., Bushnell, D.A., and Kornberg, R.D. (2004). Structural basis of transcription: separation of RNA from DNA by RNA polymerase II. Science *303*, 1014–1016.

Woudstra, E.C., Gilbert, C., Fellows, J., Jansen, L., Brouwer, J., Erdjument-Bromage, H., Tempst, P., and Svejstrup, J.Q. (2002). A Rad26-Def1 complex coordinates repair and RNA pol II proteolysis in response to DNA damage. Nature *415*, 929–933.

Wu, X., Li, J., Li, X., Hsieh, C.L., Burgers, P.M., and Lieber, M.R. (1996). Processing of branched DNA intermediates by a complex of human FEN-1 and PCNA. Nucleic Acids Res. *24*, 2036–2043.

Yu, A., Fan, H.Y., Liao, D., Bailey, A.D., and Weiner, A.M. (2000). Activation of p53 or loss of the Cockayne syndrome group B repair protein causes metaphase fragility of human U1, U2, and 5S genes. Mol. Cell *5*, 801–810.